



# The Dynamics of Local Bifurcation in a Novel Four-dimensional Hyperchaotic System

Ali Hassan\*<sup>1</sup> , Liangqiang Zhou<sup>1</sup> , Abid Hussain<sup>2</sup> , Albert Kabbah<sup>1</sup>  and Muhammad Amad Sarwar<sup>1</sup> 

<sup>1</sup> School of Mathematics, Nanjing University of Aeronautics and Astronautics, Nanjing 210016, China

<sup>2</sup> College of Aerospace Engineering, Nanjing University of Aeronautics and Astronautics, Nanjing 210016, China

\*Corresponding author: [ali.hassan3512@hotmail.com](mailto:ali.hassan3512@hotmail.com)

Received: May 8, 2024

Accepted: August 12, 2024

**Abstract.** This paper reports the findings of a novel four-dimensional autonomous quadratic hyperchaotic system characterized by three nonlinear terms. This system is developed by introducing nonlinear state feedback into the second equation of the three-dimensional Yang chaotic system. A comprehensive dynamical study follows the presentation of the mathematical model. The study includes dissipation and symmetry, stability of equilibrium points, and dynamic behaviors such as the Lyapunov exponent spectrum, bifurcation diagram, Poincaré maps, and orbits. The Poincaré-Andronov-Hopf bifurcation theorem and center manifold theory are used in local bifurcation analysis to investigate pitchfork and Hopf bifurcation at zero equilibrium points. Numerical simulations have confirmed the mathematical discoveries.

**Keywords.** Hyperchaotic system, Center manifold theorem, Local bifurcation

**Mathematics Subject Classification (2020).** 37G05, 37G15, 37G35, 37C75

Copyright © 2024 Ali Hassan, Liangqiang Zhou, Abid Hussain, Albert Kabbah and Muhammad Amad Sarwar. This is an open access article distributed under the Creative Commons Attribution License, which permits unrestricted use, distribution, and reproduction in any medium, provided the original work is properly cited.

## 1. Introduction

Chaos is often observed in nature and is a challenging dynamic event in nonlinear systems. Scholars from various areas and fields have shown significant interest in chaos theory and its applications (Biban *et al.* [2], and Yang *et al.* [18]). The Lorenz attractor [8] is an important scientific discovery that provided a foundation for the emerging theory in the field of chaos science, as it is the first classical chaotic attractor of chaos. The whole development of chaos

science is associated with the study of Lorenz-type systems. Hyperchaos, in comparison to chaos, is frequently regarded as a chaotic dynamical system characterized by having two or more positive Lyapunov exponents (LEs), which may increase the nonlinear system's instability and unpredictability. Thus, it is more beneficial to develop a novel hyperchaotic system with unique dynamical characteristics.

Since 4D autonomous systems are the lowest dimension at which hyperchaos may occur in an autonomous system, as we all know, 4D autonomous systems are the focus of most hyperchaos research and applications. In 1979, Rossler [11] identified and examined the revolutionary hyperchaotic system. Later investigations led to the discovery and study of several four-dimensional hyperchaotic systems, such as the hyperchaotic Lü system (Chen *et al.* [4]), the hyperchaotic Chua system (Rech and Albuquerque [10]), the hyperchaotic Chen system (Yuxia *et al.* [21]), the hyperchaotic Lorenz system (Al-Khedhairi *et al.* [1]), and the hyperchaotic Jia system [5], particularly four-dimensional hyperchaotic Lorenz-type systems (Chen and Yang [3], and Li *et al.* [6]). Hyperchaotic systems show a higher potential for use in encrypted communications (Yu *et al.* [20]), nonlinear circuits (Yilmaz *et al.* [19]), image encryption (Xu *et al.* [15]), and a variety of other fields compared with classical chaos systems.

Research on the bifurcation of fixed points in chaotic systems, such as pitchfork, Hopf, and homoclinic bifurcations, has been the focus of many studies in the last few years (Liu *et al.* [7], and Yan *et al.* [16]). Particularly, important types of static and dynamic bifurcations at equilibrium points include pitchfork and Hopf bifurcations. It is beneficial for real-world applications to fully investigate these bifurcations because they provide further understanding of the dynamic development of nonlinear systems. However, such bifurcation analyses in hyperchaotic systems have been less studied due to their higher dimensionality and increased complexity. Studying the bifurcation events in hyperchaotic systems therefore offers an important and relevant field of research.

The rest of the sections in this paper are presented as follows: Section 2 introduces the new hyperchaotic system and its significant dynamical features. Section 3 investigates the analysis of the Hopf and pitchfork bifurcations in the new hyperchaotic system using the center manifold theorem, bifurcation theory, and numerical simulations. In the end, the results are concisely presented in Section 4.

## 2. The Novel Hyperchaotic System and Its Dynamical Analysis

### 2.1 Mathematical Model

Yang and Chen [17] have developed a complex three-dimensional chaotic system. It can be characterized by the following equations:

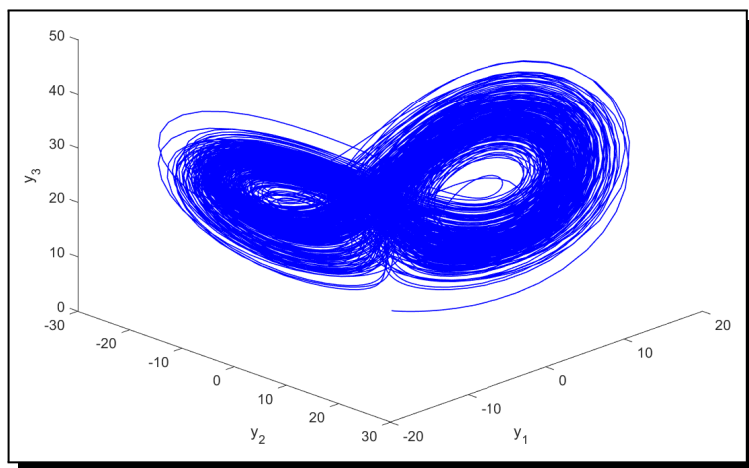
$$\begin{cases} \dot{y}_1 = \sigma(y_2 - y_1), \\ \dot{y}_2 = \rho y_1 - y_1 y_3, \\ \dot{y}_3 = -\gamma y_3 + y_1 y_2, \end{cases} \quad (1)$$

where  $\sigma, \gamma, \rho$  are real parameters, with  $\sigma > 0$ ,  $\gamma > 0$  and  $\rho \in R$ . When  $(\sigma, \gamma, \rho) = (10, 8/3, 16)$ ,  $(\sigma, \gamma, \rho) = (35, 3, 35)$ , system (1) has a chaotic attractor. By introducing an additional state variable into the set of equations in (1), the following novel 4D hyperchaotic system is proposed

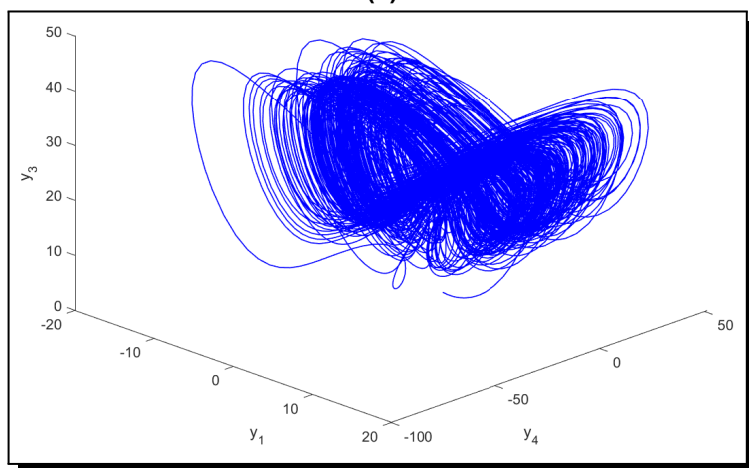
as follows:

$$\begin{cases} \dot{y}_1 = \sigma(y_2 - y_1), \\ \dot{y}_2 = \rho y_1 - y_1 y_3 + y_4, \\ \dot{y}_3 = -\gamma y_3 + y_1 y_2, \\ \dot{y}_4 = -m y_1 + n y_2 y_3, \end{cases} \tag{2}$$

where  $\sigma, \gamma, \rho, m,$  and  $n$  are the parameters of the system, and  $y_1, y_2, y_3,$  and  $y_4$  are the state variables. As shown in Figure 1, system (2) exhibits a hyperchaotic attractor with parameters  $(\sigma, \gamma, \rho, m, n) = (10, 8/3, 22, 8, 0.01)$ .



(a)



(b)

**Figure 1.** Diagram of hyperchaotic attractors in system (2) with parameters  $\sigma = 10, \gamma = 8/3, \rho = 22, m = 8$  and  $n = 0.01$

### 2.2 Symmetry and Dissipation

Given the coordinate transformation  $(y_1, y_2, y_3, y_4) \rightarrow (-y_1, -y_2, y_3, -y_4)$ , the system given in (2) keeps its form, showing that it is symmetrical with regard to the  $y_3$ -axis.

The divergence in system (2) can be obtained as follows:

$$\nabla V = \frac{\partial y_1}{\partial y_1} + \frac{\partial y_2}{\partial y_2} + \frac{\partial y_3}{\partial y_3} + \frac{\partial y_4}{\partial y_4} = -(\sigma + \gamma).$$

According to studies by Owolabi and Atangana [9] and Tarasov [12], the Lyapunov exponents of the system can be used to determine its dissipation. A system is classified as dissipative if the sum of all its Lyapunov exponents is negative. When  $\sigma = 10$ ,  $\gamma = 8/3$ ,  $\rho = 22$ ,  $m = 8$  and  $n = 0.01$ ,  $\sum_i^4 LE_i = -12.67 < 0$ , which confirms that system (2) is dissipative.

### 2.3 The Complexity of Dynamic Behaviors

Given the values  $\sigma = 10$ ,  $\gamma = 8/3$ ,  $m = 8$ ,  $n = 0.01$  and a variable  $\rho$ , we analyze the dynamic characteristics of system (2) by using the Lyapunov exponent spectrum, bifurcation diagram, and Poincaré map. The analyses can be seen in Figures 2 and 3, respectively.

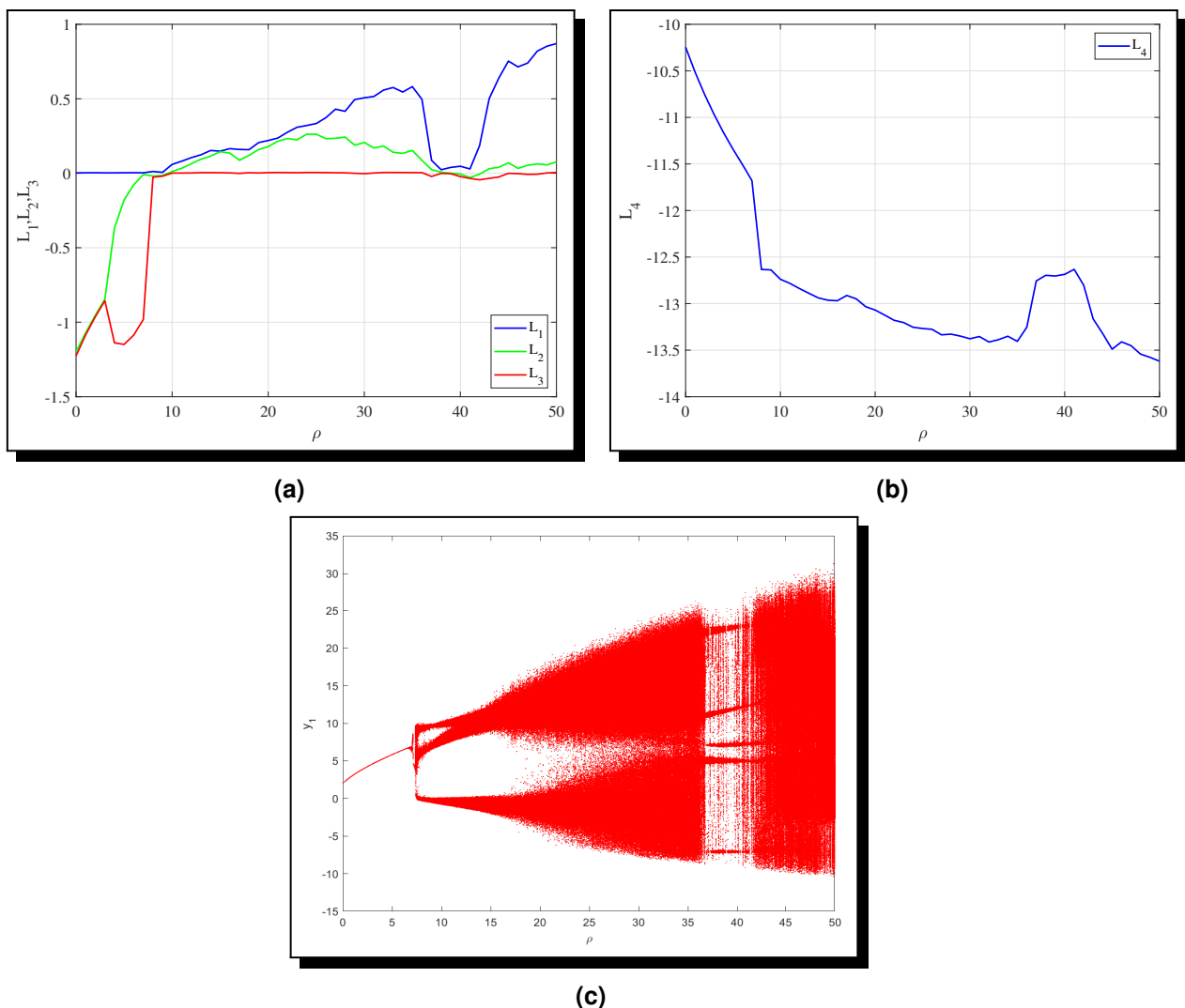


**Figure 2.** Spectrum of Lyapunov exponents and bifurcation diagram for  $\rho \in [0, 50]$ , with parameters  $\sigma = 10$ ,  $\gamma = 8/3$ ,  $m = 8$ , and  $n = 0.01$

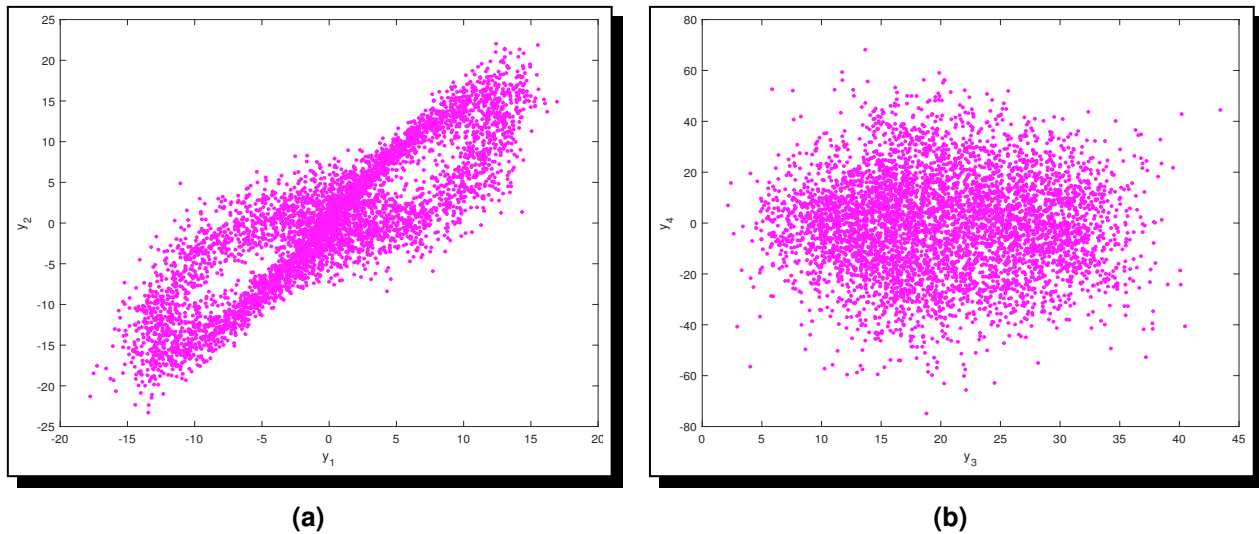


**Figure 3.** The Poincaré maps for the  $y_1$ - $y_2$  and  $y_3$ - $y_4$  planes are shown, with parameters  $\sigma = 10$ ,  $\gamma = 8/3$ ,  $\rho = 22$ ,  $m = 8$ , and  $n = 0.01$

### 2.4 The Study of Stability at Equilibrium Points

Consider the following algebraic equations to determine the equilibrium of system (2):

$$\begin{cases} \sigma(y_2 - y_1) = 0, \\ \rho y_1 - y_1 y_3 + y_4 = 0, \\ -\gamma y_3 + y_1 y_2 = 0, \\ -m y_1 + n y_2 y_3 = 0. \end{cases} \tag{3}$$

It can be observed that system (2) has an origin equilibrium point,  $EQ_1 = (0,0,0,0)$ . In addition, when  $mn\gamma > 0$ , system (2) shows two more equilibrium points:  $EQ_2 = \left(\frac{\sqrt{mn\gamma}}{n}, \frac{\sqrt{mn\gamma}}{n}, \frac{m}{n}, \frac{(m-\rho n)\sqrt{mn\gamma}}{n^2}\right)$  and  $EQ_3 = \left(-\frac{\sqrt{mn\gamma}}{n}, -\frac{\sqrt{mn\gamma}}{n}, \frac{m}{n}, -\frac{(m-\rho n)\sqrt{mn\gamma}}{n^2}\right)$ . The next section will provide a concise overview of the stability of the origin equilibrium  $EQ_1$ . The Jacobian matrix evaluated at  $EQ_1$  is

$$J_{EQ_1} = \begin{bmatrix} -\sigma & \sigma & 0 & 0 \\ \rho & 0 & 0 & 1 \\ 0 & 0 & -\gamma & 0 \\ -m & 0 & 0 & 0 \end{bmatrix}. \tag{4}$$

Subsequently, we derive the associated characteristic equation as

$$\phi(\lambda) = (\lambda + \gamma) \cdot \phi^1(\lambda) = 0, \tag{5}$$

where

$$\phi^1(\lambda) = (\lambda^3 + \sigma\lambda^2 - \sigma\rho\lambda + \sigma m). \tag{6}$$

Certainly,  $-\gamma$  is a root of equation (5). According to Routh-Hurwitz criteria, the remaining three roots may not consistently contain the negative real part. Section 3 will focus on the analysis of the bifurcation phenomena, specifically in the case where the zero equilibrium is non-hyperbolic.

### 3. Local Bifurcation Analysis

#### 3.1 Pitchfork Bifurcation

We take  $m$  as a bifurcation parameter in the following investigation. The eigenvalues of Jacobian matrix (4) when  $m = 0$  are given by  $\lambda_1 = 0$ ,  $\lambda_2 = -\gamma$ ,  $\lambda_{3,4} = \frac{-\sigma \pm \sqrt{\sigma(\sigma+4\rho)}}{2}$ , with the associated eigenvectors

$$v_1 = \begin{bmatrix} -1 \\ -1 \\ 0 \\ \rho \end{bmatrix}, \quad v_2 = \begin{bmatrix} 0 \\ 0 \\ 1 \\ 0 \end{bmatrix}, \quad v_3 = \begin{bmatrix} \frac{-(\sigma + \sqrt{\sigma(\sigma+4\rho)})}{2\rho} \\ 1 \\ 0 \\ 0 \end{bmatrix}, \quad v_4 = \begin{bmatrix} \frac{-(\sigma - \sqrt{\sigma(\sigma+4\rho)})}{2\rho} \\ 1 \\ 0 \\ 0 \end{bmatrix}.$$

Thus, the equilibrium  $EQ_1 = (0, 0, 0, 0)$  is not hyperbolic, and we will analyze the stability of the equilibrium point  $EQ_1 = (0, 0, 0, 0)$  close to the bifurcation point  $m = 0$  by using the center manifold theorem (Wiggins [14]).

Firstly, describe a transformation, which is

$$\begin{bmatrix} y_1 \\ y_2 \\ y_3 \\ y_4 \end{bmatrix} = \begin{bmatrix} x_1 \\ x_2 \\ x_3 \\ x_4 \end{bmatrix}, \tag{7}$$

where

$$T = (v_1, v_2, v_3, v_4) = \begin{bmatrix} -1 & 0 & \frac{-(\sigma+q)}{2\rho} & \frac{-(\sigma-q)}{2\rho} \\ -1 & 0 & 1 & 1 \\ 0 & 1 & 0 & 0 \\ \rho & 0 & 0 & 0 \end{bmatrix}, \tag{8}$$

and  $q = \sqrt{\sigma(\sigma+4\rho)}$ .

Thus, system (2) can be changed into the following system:

$$\begin{bmatrix} \dot{x}_1 \\ \dot{x}_2 \\ \dot{x}_3 \\ \dot{x}_4 \end{bmatrix} = \begin{bmatrix} 0 & 0 & 0 & 0 \\ 0 & -\gamma & 0 & 0 \\ 0 & 0 & \frac{-\sigma+q}{2} & 0 \\ 0 & 0 & 0 & \frac{-\sigma-q}{2} \end{bmatrix} \begin{bmatrix} x_1 \\ x_2 \\ x_3 \\ x_4 \end{bmatrix} + \begin{bmatrix} \Phi_1 \\ \Phi_2 \\ \Phi_3 \\ \Phi_4 \end{bmatrix}, \tag{9}$$

where

$$\begin{aligned} \Phi_1 &= \frac{m}{\rho}x_1 + \frac{m(\sigma+q)}{2\rho^2}x_3 + \frac{m(\sigma-q)}{2\rho^2}x_4 + \frac{n(x_3-x_1+x_4)x_2}{\rho}, \\ \Phi_2 &= -(x_3-x_1+x_4)\left(x_1 + \frac{\sigma+q}{2\rho}x_3 + \frac{\sigma-q}{2\rho}x_4\right), \\ \Phi_3 &= -\frac{m(\sigma+2\rho-q)}{2\rho q}x_1 - \frac{m(\sigma+q)(\sigma+2\rho-q)}{4q\rho^2}x_3 - \frac{m(\sigma-q)(\sigma+2\rho-q)}{4q\rho^2}x_4 \\ &\quad - \frac{n(\sigma+2\rho-q)(x_3-x_1+x_4)x_2}{2\rho q} - \frac{(\sigma-q)\left(x_1 + \frac{\sigma+q}{2\rho}x_3 + \frac{\sigma-q}{2\rho}x_4\right)x_2}{2q}, \\ \Phi_4 &= \frac{m(\sigma+2\rho+q)}{2\rho q}x_1 + \frac{m(\sigma+q)(\sigma+2\rho+q)}{4q\rho^2}x_3 + \frac{m(\sigma-q)(\sigma+2\rho+q)}{4q\rho^2}x_4 \end{aligned}$$

$$+ \frac{n(\sigma + 2\rho + q)(x_3 - x_1 + x_4)x_2}{2\rho q} + \frac{(\sigma + q)(x_1 + \frac{\sigma+q}{2\rho}x_3 + \frac{\sigma-q}{2\rho}x_4)x_2}{2q}.$$

Hence, the stability of the point  $EQ_1 = (0, 0, 0, 0)$  close to  $m = 0$  can be discovered by using center manifold theory. This involves investigating a set of 1st-order fundamental ordinary differential equations (ODEs) with a single parameter on a center manifold. The equations can be graphically represented by plotting the variables  $x_1$  and  $m$  on a graph as follows:

$$W_c(0) = \left\{ (x_1, x_2, x_3, x_4, m) \in \mathbb{R}^5 \left| \begin{array}{l} x_2 = h_1(x_1, m), \ x_3 = h_2(x_1, m), \ x_4 = h_3(x_1, m), \\ |x_1| < \theta, \ |m| < \bar{\theta}, \\ h_i(0, 0) = 0, \ Dh_i(0, 0) = 0, \ i = 1, 2, 3 \end{array} \right. \right\} \tag{10}$$

where both  $\theta$  and  $\bar{\theta}$  be sufficiently small.

To calculate the center manifold and to obtain the vector field associated with it, consider that

$$\begin{cases} x_2 = h_1(x_1, m) = a_1x_1^2 + a_2x_1m + a_3m^2 + \dots, \\ x_3 = h_2(x_1, m) = b_1x_1^2 + b_2x_1m + b_3m^2 + \dots, \\ x_4 = h_3(x_1, m) = c_1x_1^2 + c_2x_1m + c_3m^2 + \dots \end{cases} \tag{11}$$

Recall that the center manifold needs to meet [14]

$$N(h(x_1, m)) = Dh \cdot \Phi_1 - Bh - \Phi = 0, \tag{12}$$

where

$$h = \begin{bmatrix} h_1 \\ h_2 \\ h_3 \end{bmatrix}, \quad \Phi = \begin{bmatrix} \Phi_2 \\ \Phi_3 \\ \Phi_4 \end{bmatrix}, \quad B = \begin{bmatrix} -\gamma & 0 & 0 \\ 0 & \frac{-\sigma+q}{2} & 0 \\ 0 & 0 & \frac{-\sigma-q}{2} \end{bmatrix}. \tag{13}$$

By using the expression (11) in equation (12) and combining the expression (13), one can obtain that

$$\begin{aligned} x_1^2 : \gamma a_1 - 1 = 0 &\implies a_1 = \frac{1}{\gamma}, \ b_1 = 0, \ c_1 = 0, \\ x_1m : a_2 = 0, \ -\left(\frac{-\sigma+q}{2}\right)b_2 - \left(-\frac{\sigma+2\rho-q}{2\rho q}\right) &= 0, \\ \implies b_2 = -\frac{\sigma+2\rho-q}{\rho q(\sigma-q)}, \ c_2 = \frac{\sigma+2\rho+q}{\rho q(\sigma+q)}, \\ m^2 : a_3 = 0, \ b_3 = 0, \ c_3 = 0. \end{aligned} \tag{14}$$

As a result, equation (11) can be rewritten as

$$\begin{cases} x_2 = h_1(x_1, m) = a_1x_1^2 + \dots, \\ x_3 = h_2(x_1, m) = b_2x_1m + \dots, \\ x_4 = h_3(x_1, m) = c_2x_1m + \dots \end{cases} \tag{15}$$

Hence, a reduced vector field is derived by substituting eq. (15) into  $\dot{x}_1 = \Phi_1$  of eq. (9), and one can obtain:

$$\left. \begin{aligned} \dot{x}_1 &= \frac{1}{\rho}x_1m - \frac{(\sigma+q)}{2\rho^2} \cdot \frac{(\sigma+2\rho-q)}{\rho q(\sigma-q)}x_1m^2 + \frac{(\sigma-q)}{2\rho^2} \cdot \frac{(\sigma+2\rho+q)}{\rho q(\sigma+q)}x_1m^2 - \frac{n}{\rho\gamma}x_1^3 + o(x_1^4), \\ \dot{m} &= 0. \end{aligned} \right\} \tag{16}$$

Suppose

$$H(x_1, m) = \frac{1}{\rho}x_1m - \frac{(\sigma + q)}{2\rho^2} \cdot \frac{(\sigma + 2\rho - q)}{\rho q(\sigma - q)}x_1m^2 + \frac{(\sigma - q)}{2\rho^2} \cdot \frac{(\sigma + 2\rho + q)}{\rho q(\sigma + q)}x_1m^2 - \frac{n}{\rho\gamma}x_1^3.$$

By the pitchfork bifurcation theory [14], it is simple to verify that the following requirements are fulfilled. Consequently, system (16) experiences a pitchfork bifurcation at  $(x_1, m) = (0, 0)$  when  $m = 0$ . As  $-\frac{\partial^3 H}{\partial x_1^3} / \frac{\partial^2 H}{\partial x_1 \partial m} > 0$ , the direction of the bifurcation is towards  $m > 0$ .

$$\begin{aligned} H(0, 0) &= 0, & \frac{\partial H}{\partial x_1} \Big|_{(0,0)} &= 0, & \frac{\partial H}{\partial m} \Big|_{(0,0)} &= 0, & \frac{\partial^2 H}{\partial x_1^2} \Big|_{(0,0)} &= 0, \\ \frac{\partial^2 H}{\partial x_1 \partial m} \Big|_{(0,0)} &= \frac{1}{\rho} \neq 0, & \frac{\partial^3 H}{\partial x_1^3} \Big|_{(0,0)} &= \frac{-6n}{\rho\gamma} \neq 0. \end{aligned}$$

Thus, Theorem 1 can be derived.

**Theorem 1.** *When  $m = 0$ , system (2) experiences a pitchfork bifurcation at  $EQ_1 = (0, 0, 0, 0)$ . Moreover, for  $m < 0$ , there exists a single origin equilibrium point  $EQ_1 = (0, 0, 0, 0)$  that is locally stable and located on the left of  $m = 0$ .  $EQ_1 = (0, 0, 0, 0)$  becomes unstable when  $m > 0$ , and the remaining two equilibrium points  $EQ_2 = (\sqrt{mn\gamma}/n, \sqrt{mn\gamma}/n, m/n, (m - \rho n)\sqrt{mn\gamma}/n^2)$  and  $EQ_3 = (-\sqrt{mn\gamma}/n, -\sqrt{mn\gamma}/n, m/n, -(m - \rho n)\sqrt{mn\gamma}/n^2)$  appear and become locally stable close to the right side of  $m = 0$ .*

### 3.2 Hopf Bifurcation

Consider a vector field:

$$\dot{y} = g(y, \eta), \quad y \in \mathbb{R}^n, \eta \in \mathbb{R}. \tag{17}$$

If all three of the following criteria are met simultaneously by the vector field [13], it will experience a Hopf bifurcation.

(C1):  $g(y_0, \eta_0) = 0$ , the Jacobian matrix  $Dg(y_0, \eta_0)$  has two purely imaginary eigenvalues,  $\phi_1(\eta_0)$  and  $\phi_2(\eta_0)$ .

(C2): Transversality condition: the real parts of eigenvalues satisfy

$$\left. \frac{d}{d\eta}(\text{Re}(\phi_{1,2}(\eta))) \right|_{\eta=\eta_0} \neq 0.$$

(C3): The index number  $\Lambda_0$  is nonzero.

Next, we will examine each of the three listed criteria individually. Let's start by assuming that it has two eigenvalues  $\lambda = \pm iw_0$ , where  $w_0$  is a positive real number. By placing one of the eigenvalues into equation (6), we can obtain the following expression:

$$-w_0^3 i - \sigma w_0^2 - \sigma \rho w_0 i + \sigma m = 0. \tag{18}$$

Eq. (18) can be expressed as:

$$\begin{cases} -w_0^3 - \sigma \rho w_0 = 0, \\ \sigma m - \sigma w_0^2 = 0. \end{cases} \tag{19}$$

The solution of equation (19) yields  $\rho = -\frac{m}{\sigma}$  and  $w_0 = \sqrt{m}$ , where  $m > 0$ .

Hence, by substituting  $\rho = -\frac{m}{\sigma}$  in equation (5), we obtain  $\lambda_1 = -\gamma$ ,  $\lambda_2 = -\sigma$ ,  $\lambda_3 = i\sqrt{m}$ ,  $\lambda_4 = -i\sqrt{m}$ , where  $\sigma \in \mathbb{R}^+$ ,  $\gamma \in \mathbb{R}^+$  and  $m > 0$ . Hence, condition (C1) is satisfied when  $\rho = -\frac{m}{\sigma}$ . Now consider the expression  $\lambda(\rho) = \alpha(\rho) + iw_0(\rho)$ , where  $\pm iw_0$  are roots of the equation  $\phi^1(\lambda) = 0$ . By substituting  $\lambda(\rho)$  into  $\phi^1(\lambda) = 0$  and applying a differentiation of both sides of equation  $\phi^1(\lambda) = 0$  with respect to  $\rho$ , we obtain

$$\frac{d\lambda(\rho)}{d\rho} = \frac{\sigma\lambda}{3\lambda^2 + 2\sigma\lambda - \sigma\rho},$$

which implies that

$$\left. \frac{d\lambda(\rho)}{d\rho} \right|_{\rho = -\frac{m}{\sigma}} = \frac{i\sigma w_0}{-3w_0^2 + 2\sigma i w_0 + m}. \tag{20}$$

Thus, we have obtained

$$\rho_1 = \text{Re}(\lambda'(\rho)) \Big|_{\rho = -\frac{m}{\sigma}} = \frac{2\sigma^2 w_0^2}{[-3w_0^2 + m]^2 + 4\sigma^2 w_0^2} = 0.5 \neq 0. \tag{21}$$

As a result, the condition (C2) is also fulfilled.

Finally, we will continue to apply the center manifold theorem in order to calculate the index number  $\Lambda_0$ , ensuring it meets the condition (C3) where  $\Lambda_0 \neq 0$ . If we look at the Jacobian matrix (4) and set  $\rho = -\frac{m}{\sigma}$ , we find the eigenvalues to be  $\lambda_1 = -\gamma$ ,  $\lambda_2 = -\sigma$ ,  $\lambda_3 = i\sqrt{m}$ , and  $\lambda_4 = -i\sqrt{m}$ , with their associated eigenvectors.

$$v_1 = \begin{bmatrix} 0 \\ 0 \\ 1 \\ 0 \end{bmatrix}, \quad v_2 = \begin{bmatrix} \sigma \\ 0 \\ 0 \\ w_0^2 \end{bmatrix}, \quad v_3 = \begin{bmatrix} c1 \\ 1 + \frac{w_0}{\sigma}i \\ 0 \\ w_0i \end{bmatrix}, \quad v_4 = \begin{bmatrix} c1 \\ 1 - \frac{w_0}{\sigma}i \\ 0 \\ -w_0i \end{bmatrix}.$$

Define the transformation as follows:

$$\begin{bmatrix} y_1 \\ y_2 \\ y_3 \\ y_4 \end{bmatrix} = Q \begin{bmatrix} z_1 \\ z_2 \\ z_3 \\ z_4 \end{bmatrix}, \tag{22}$$

where

$$Q = (\text{Re}(v_3), -\text{Im}(v_3), v_1, v_2) = \begin{bmatrix} 1 & 0 & 0 & \sigma \\ 1 & -\frac{w_0}{\sigma} & 0 & 0 \\ 0 & 0 & 1 & 0 \\ 0 & -w_0 & 0 & w_0^2 \end{bmatrix}. \tag{23}$$

System (2) can be rewritten as follows:

$$\begin{bmatrix} \dot{z}_1 \\ \dot{z}_2 \\ \dot{z}_3 \\ \dot{z}_4 \end{bmatrix} = \begin{bmatrix} 0 & -w_0 & 0 & 0 \\ w_0 & 0 & 0 & 0 \\ 0 & 0 & -\gamma & 0 \\ 0 & 0 & 0 & -\sigma \end{bmatrix} \begin{bmatrix} z_1 \\ z_2 \\ z_3 \\ z_4 \end{bmatrix} + \begin{bmatrix} f_1 \\ f_2 \\ f_3 \\ f_4 \end{bmatrix}, \tag{24}$$

where

$$f_1 = \frac{-\sigma^2(z_1 + \sigma z_4)z_3 - \sigma n(z_1 - \frac{w_0}{\sigma} z_2)z_3}{\sigma^2 + w_0^2},$$

$$f_2 = \frac{\sigma w_0(z_1 + \sigma z_4)z_3 - \sigma^2 n\left(\frac{1}{w_0}z_1 - \frac{1}{\sigma}z_2\right)z_3}{\sigma^2 + w_0^2},$$

$$f_3 = (z_1 + \sigma z_4)\left(z_1 - \frac{w_0}{\sigma}z_2\right),$$

$$f_4 = \frac{n\left(z_1 - \frac{w_0}{\sigma}z_2\right)z_3 + \sigma(z_1 + \sigma z_4)z_3}{\sigma^2 + w_0^2}.$$

Equation (24) can be rewritten as follows:

$$\begin{cases} \dot{U} = AU + f(U, V), \\ \dot{V} = BV + g(U, V), \end{cases} \tag{25}$$

where

$$\begin{cases} A = \begin{bmatrix} 0 & -w_0 \\ w_0 & 0 \end{bmatrix}, & B = \begin{bmatrix} -\gamma & 0 \\ 0 & -\sigma \end{bmatrix}, & U = \begin{bmatrix} z_1 \\ z_2 \end{bmatrix}, & V = \begin{bmatrix} z_3 \\ z_4 \end{bmatrix}, \\ f(U, V) = \begin{bmatrix} f_1 \\ f_2 \end{bmatrix}, & g(U, V) = \begin{bmatrix} f_3 \\ f_4 \end{bmatrix}. \end{cases} \tag{26}$$

According to center manifold theory, a center manifold exists for equation (25) and can be represented as

$$W_c(0) = \{(U, V) \in \mathbb{R}^2 \times \mathbb{R}^2 \mid V = h(U), |U| < \theta, h(0, 0) = 0, Dh(0, 0) = 0\}, \tag{27}$$

where  $\theta$  is sufficiently small and

$$h(U) = \begin{bmatrix} h_1(U) \\ h_2(U) \end{bmatrix} = \begin{bmatrix} h_1(z_1, z_2) \\ h_2(z_1, z_2) \end{bmatrix}. \tag{28}$$

We assume that  $z_3 = h_1(z_1, z_2)$  and  $z_4 = h_2(z_1, z_2)$  have the forms as follows:

$$\begin{cases} z_3 = h_1(z_1, z_2) = d_1z_1^2 + d_2z_1z_2 + d_3z_2^2 + \dots, \\ z_4 = h_2(z_1, z_2) = e_1z_1^2 + e_2z_1z_2 + e_3z_2^2 + \dots \end{cases} \tag{29}$$

According to center manifold theory [14], the center manifold has to meet

$$Dh(U)[AU + f(U, V)] - Bh(U) - g(U, V) = 0. \tag{30}$$

Substituting eq. (26) to eq. (30), expression (27) and equations (29) can be utilized to compare and balance the coefficients of the identical terms  $(z_1^2, z_1z_2, z_2^2)$ , resulting in the following:

$$\begin{cases} z_1^2 & : d_2w_0 + \gamma d_1 - 1 = 0, e_2w_0 + \sigma e_1 = 0, \\ z_1z_2 & : -2d_1w_0 + 2d_3w_0 + \gamma d_2 + \frac{w_0}{\sigma} = 0, \\ & -2e_1w_0 + 2e_3w_0 + \sigma e_2 = 0, \\ z_2^2 & : -d_2w_0 + \gamma d_3 = 0, -e_2w_0 + \sigma e_3 = 0. \end{cases} \tag{31}$$

Then the following solution can be obtained:

$$d_1 = \frac{\gamma + \frac{w_0^2}{\sigma} + \frac{2w_0^2}{\gamma}}{\gamma^2 + 4w_0^2}, \quad d_2 = \frac{2w_0 - \frac{\gamma w_0}{\sigma}}{\gamma^2 + 4w_0^2}, \quad d_3 = \frac{\frac{2}{\gamma}w_0^2 - \frac{w_0}{\sigma}}{\gamma^2 + 4w_0^2}. \tag{32}$$

Therefore,  $f_1$  and  $f_2$  may be expressed as

$$\begin{cases} f^1 = \frac{1}{\sigma^2+w_0^2}[-\sigma^2 z_1 - \sigma n z_1 + n w_0 z_2](d_1 z_1^2 + d_2 z_1 z_2 + d_3 z_2^2 + \dots), \\ f^2 = \frac{1}{\sigma^2+w_0^2}[\sigma w_0 z_1 - \frac{\sigma^2 n}{w_0} z_1 + \sigma n z_2](d_1 z_1^2 + d_2 z_1 z_2 + d_3 z_2^2 + \dots). \end{cases} \tag{33}$$

Thus, we can apply the following formula to calculate the index number  $\Lambda_0$ :

$$\begin{aligned} \Lambda_0 &= \frac{1}{16}(f_{z_1 z_1 z_1}^1 + f_{z_1 z_2 z_2}^1 + f_{z_1 z_1 z_2}^2 + f_{z_2 z_2 z_2}^2) \\ &\quad + \frac{1}{16 w_0}[f_{z_1 z_2}^1(f_{z_1 z_1}^1 + f_{z_2 z_2}^1) - f_{z_1 z_2}^2(f_{z_1 z_1}^2 + f_{z_2 z_2}^2) - f_{z_1 z_1}^1 f_{z_1 z_1}^2 + f_{z_2 z_2}^1 f_{z_2 z_2}^2] \\ &= \frac{1}{8(\sigma^2 + w_0^2)} \left\{ [\sigma n - 3(\sigma^2 + n\sigma)]d_1 + \left[ n w_0 + \sigma w_0 - \frac{\sigma^2 n}{w_0} \right] d_2 + [3\sigma n - (\sigma^2 + n\sigma)]d_3 \right\}. \end{aligned} \tag{34}$$

**Theorem 2.** *In a novel system, a Hopf bifurcation occurs at the origin equilibrium point,  $EQ_1 = (0, 0, 0, 0)$ , when conditions (C1) and (C2) are satisfied and  $\Lambda_0 \neq 0$  in equation (34). This bifurcation leads to the emergence of a periodic orbit close to  $\rho_0 = -m/\sigma$ . This orbit is considered stable if  $\Lambda_0 < 0$ , but it becomes unstable when  $\Lambda_0 > 0$ . The direction of the bifurcation is above (below)  $\rho_0$  depending on whether  $\rho_1 \Lambda_0$  is less than (greater than) 0.*

### 3.3 Numerical Simulations

Numerical simulations are performed in this subsection to verify the validity of Theorems 1 and 2 for both pitchfork and Hopf bifurcation. The simulation uses constant parameters:  $\sigma = 10$ ,  $\gamma = 8/3$ ,  $\rho = 27$ ,  $m = 8$ , and  $n = 0.2$ . In Section 3.1, it is important to note that the pitchfork bifurcation occurs at  $m = 0$ . Similarly, in Section 3.2, the Hopf bifurcation takes place at  $\rho_0 = -\frac{m}{\sigma}$ . The given parameters are  $\rho = \rho_0 = -0.8$ ,  $\Lambda_0 = -0.086$ , and  $\rho_1 \Lambda_0 < 0$ .

According to Theorem 1, system 2 would experience a pitchfork bifurcation at  $EQ_1$  when  $m = 0$ . Thus, there would be a change in both the number and stability of the equilibria around the value of  $m = 0$ . The system should have two stable nonzero equilibrium points,  $EQ_2$  and  $EQ_3$ , and one unstable zero equilibrium point,  $EQ_1$ , nearby to the right of  $m = 0$ . In the left part of  $m = 0$ , there should only be one stable zero equilibrium point,  $EQ_1$ . The  $x_1$ -coordinate values of fixed locations in the surrounding area of  $m = 0$ , ranging from  $-4$  to  $4$ , are displayed in Figure 4. Figure 4 illustrates that the bifurcation direction occurs when  $m > 0$ . While  $EQ_1$  is stable for  $m < 0$ , it becomes unstable and is replaced by the stable states  $EQ_2$  and  $EQ_3$  when  $m > 0$ . This observation corresponds to the result derived from Theorem 1.

According to Theorem 2, the bifurcation direction is above  $\rho_0$ , and the limit cycle close to  $\rho_0$  should be stable. The provided numerical simulations serve to verify the outcomes of the theorem. In Figure 5(a), the trajectory of system (2) is drawn towards the stable origin equilibrium point  $EQ_1$  by choosing the value of  $\rho$  as  $-0.9$ , which is located in the left region of  $\rho_0$ . In Figure 5(b), the trajectory of system 2 is drawn towards a stable limit cycle that derives from  $EQ_1$  by choosing the value of  $\rho$  as  $-0.6$ , which is in close range to  $\rho_0$ . The simulation findings clearly support the conclusion drawn from Theorem 2.

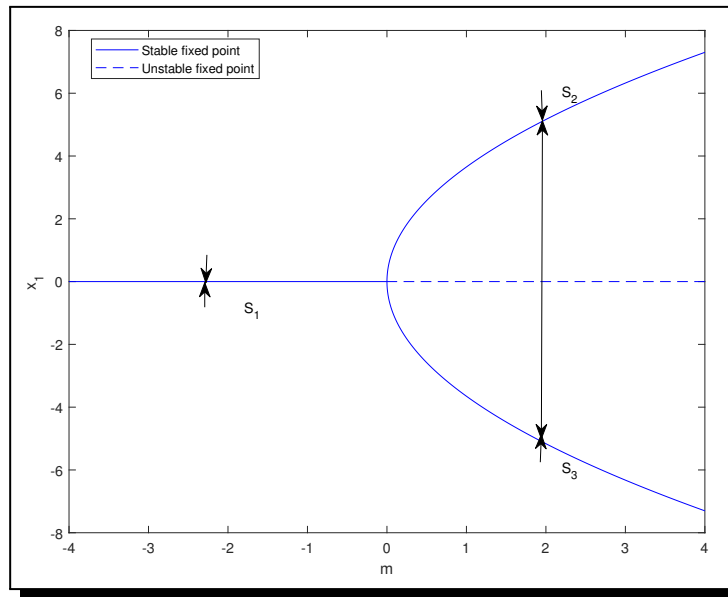


**Figure 4.** Pitchfork bifurcation diagram of system (2) at  $m = 0$

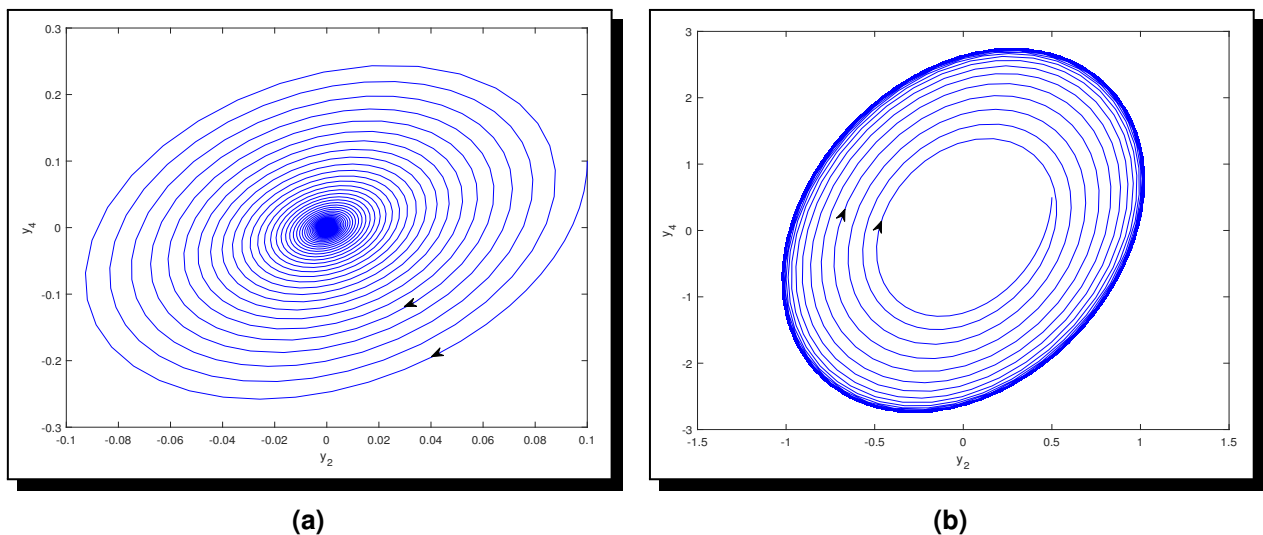


**Figure 5.** (a)  $\rho = -0.9 < \rho_0$ , the system’s trajectory converges to a stable origin equilibrium point,  $EQ_1$ . (b)  $\rho = -0.6 > \rho_0$ , the system’s trajectory evolves towards a stable limit cycle arises from  $EQ_1$

### 4. Conclusions

This paper introduces a novel type of hyperchaotic system having four coupled ordinary differential equations with three quadratic nonlinear parts in a continuous time frame. A variety of dynamic behaviors, including the Lyapunov exponent spectrum, bifurcation diagrams, and Poincaré maps, have been shown by the comprehensive dynamical analysis that was conducted. The system has also shown stability at equilibrium points, symmetry, and dissipation properties. The Poincaré-Andronov-Hopf bifurcation theorem and center manifold theory have been used in local bifurcation investigations to show pitchfork and Hopf bifurcations at zero equilibrium points. Combining mathematical results with numerical simulations validates the flexibility of the proposed hyperchaotic system.

## Acknowledgments

The research is supported by the National Natural Science Foundation of China (Nos. 11772148, 12172166).

## Competing Interests

The authors declare that they have no competing interests.

## Authors' Contributions

All the authors contributed significantly in writing this article. The authors read and approved the final manuscript.

## References

- [1] A. Al-Khedhairi, A. Elsonbaty, A. H. A. Kader and A. A. Elsadany, Dynamic analysis and circuit implementation of a new 4D Lorenz-type hyperchaotic system, *Mathematical Problems in Engineering* **2019**(1) (2019), 6581586, DOI: 10.1155/2019/6581586.
- [2] G. Biban, R. Chugh and A. Panwar, Image encryption based on 8D hyperchaotic system using Fibonacci Q-Matrix, *Chaos, Solitons & Fractals* **170** (2023), 113396, DOI: 10.1016/j.chaos.2023.113396.
- [3] Y. Chen and Q. Yang, A new Lorenz-type hyperchaotic system with a curve of equilibria, *Mathematics and Computers in Simulation* **112** (2015), 40 – 55, DOI: 10.1016/j.matcom.2014.11.006.
- [4] A. Chen, J. Lu, J. Lü and S. Yu, Generating hyperchaotic Lü attractor via state feedback control, *Physica A: Statistical Mechanics and its Applications* **364** (2006), 103 – 110, DOI: 10.1016/J.PHYSA.2005.09.039.
- [5] Q. Jia, Hyperchaos generated from the Lorenz chaotic system and its control, *Physics Letters A* **366**(3) (2007), 217 – 222, DOI: 10.1016/J.PHYSLETA.2007.02.024.
- [6] Y. Li, Z. Wei and A. A. Aly, A 4D hyperchaotic Lorenz-type system: zero-Hopf bifurcation, ultimate bound estimation, and its variable-order fractional network, *The European Physical Journal Special Topics* **231** (2022), 1847 – 1858, DOI: 10.1140/epjs/s11734-022-00448-2.
- [7] Y. Liu, Y. Zhou and B. Guo, Hopf bifurcation, periodic solutions, and control of a new 4D hyperchaotic system, *Mathematics* **11**(12) (2023), 2699, DOI: 10.3390/math11122699.
- [8] E. Lorenz, Deterministic nonperiodic flow, *Journal of the Atmospheric Sciences* **20**(2) (1963), 130 – 141, DOI: 10.1175/1520-0469(1963)020<0130:DNF>2.0.CO;2.
- [9] K. M. Owolabi and A. Atangana, Numerical simulations of chaotic and complex spatiotemporal patterns in fractional reaction–diffusion systems, *Computational and Applied Mathematics* **37** (2018), 2166 – 2189, DOI: 10.1007/S40314-017-0445-X.
- [10] P. C. Rech and H. A. Albuquerque, A hyperchaotic Chua system, *International Journal of Bifurcation and Chaos* **19**(11) (2009), 3823 – 3828, DOI: 10.1142/S0218127409025146.
- [11] O. E. Rossler, An equation for hyperchaos, *Physics Letters A* **71**(2-3) (1979), 155 – 157, DOI: 10.1016/0375-9601(79)90150-6.
- [12] V. E. Tarasov, Fractional integration and fractals, in: *Fractional Dynamics. Nonlinear Physical Science*, Springer, Berlin — Heidelberg (2010), pp. 3 – 48, DOI: 10.1007/978-3-642-14003-7\_1.
- [13] J. Wang, Q. Zhang, Z. Chen and H. Li, Local bifurcation analysis and ultimate bound of a novel 4D hyper-chaotic system, *Nonlinear Dynamics* **78** (2014), 2517 – 2531, DOI: 10.1007/s11071-014-1607-7.

- [14] S. Wiggins, *Introduction to Applied Nonlinear Dynamical Systems and Chaos*, 2nd edition, Texts in Applied Mathematics, Vol. 2, Springer, New York, xxxviii + 843 pages (2003), DOI: 10.1007/b97481.
- [15] C. Xu, J. Sun and C. Wang, A novel image encryption algorithm based on bit-plane matrix rotation and hyper chaotic systems, *Multimedia Tools and Applications* **79** (2020), 5573 – 5593, DOI: 10.1007/s11042-019-08273-x.
- [16] S. Yan, X. Sun, Z. Song and Y. Ren, Dynamical analysis and bifurcation mechanism of four-dimensional hyperchaotic system, *The European Physical Journal Plus* **137** (2022), article number 734, DOI: 10.1140/epjp/s13360-022-02943-w.
- [17] Q. Yang and G. Chen, A chaotic system with one saddle and two stable node-foci, *International Journal of Bifurcation and Chaos* **18**(05) (2008), 1393 – 1414, DOI: 10.1142/S0218127408021063.
- [18] J. Yang, Z. Feng and Z. Liu, A new five-dimensional hyperchaotic system with six coexisting attractors, *Qualitative Theory of Dynamical Systems* **20** (2021), article number 18, DOI: 10.1007/s12346-021-00454-0.
- [19] G. Yilmaz, K. Altun and E. Günay, Synchronization of hyperchaotic Wang-Liu system with experimental implementation on FPAA and FPGA, *Analog Integrated Circuits and Signal Processing* **113** (2022), 145 – 161, DOI: 10.1007/s10470-022-02073-4.
- [20] J. Yu, K. Peng, L. Zhang and W. Xie, Image encryption algorithm based on DNA network and hyperchaotic system, *The Visual Computer* **40** (2024), 8001 – 8021, DOI: 10.1007/s00371-023-03219-9.
- [21] L. Yuxia, K. S. T. Wallace and C. Guanrong, Generating hyperchaos via a simple periodic forcing signal, in: *Proceedings of the 2007 Chinese Control Conference, Zhangjiajie, China*, (2007), pp. 380 – 384, DOI: 10.1109/CHICC.2006.4347259.

